Angewandte Chemie

DOI: 10.1002/ange.201307286

Molecular Dynamics Simulations

Isomerization and Decomposition of a Criegee Intermediate in the Ozonolysis of Alkenes: Dynamics Using a Multireference Potential**

Jaroslaw Kalinowski, Markku Räsänen, Petri Heinonen, Ilkka Kilpeläinen, and R. Benny Gerber*

Abstract: *The isomerization and decomposition dynamics of the simplest Criegee intermediate CH_2OO have been studied by classical trajectory simulations using the multireference ab initio MR-PT2 potential on the fly. A new, accelerated algorithm for dynamics with MR-PT2 was used. For an initial temperature of 300 K, starting from the transition state from $CH_2OO \rightarrow CH_2O_2$, the system reaches the dioxirane structure in around 50 fs, then isomerizes to formic acid (in ca. 2800 fs), and decomposes into $CO + H_2O$ at around 2900 fs. The contributions of different configurations to the multiconfigurational total electronic wave function vary dramatically along the trajectory, with diradical contributions being important for transition states corresponding to H-atom transfers, while being only moderately significant for CH_2OO. The implications for reactions of Criegee intermediates are discussed.*

The reactions of ozone with alkenes have been the topic of extensive studies for many years. A widely accepted qualitative mechanism for these reactions was suggested by Criegee and co-workers in 1949.[1] Criegee proposed that the ozonolysis of alkenes proceeds through diradical carbonyl oxides. Since then, many experimental and computational studies have been carried out to understand the properties of the so-called Criegee intermediates and elucidate their role in various chemical environments.[2,3] In particular, these species are currently of major interest in atmospheric chemistry.[4,5] Important progress was made in synthesizing Criegee intermediates in the laboratory, for example, by using the reaction $CH_2I + O_2 \rightarrow CH_2IOO \rightarrow CH_2OO + I$.[6–8] The spectroscopic properties of several Criegee intermediates were measured,[9–11] and a number of quantum chemical calculations were carried out to understand the electronic structure and chemical bonding of the carbonyl oxides.[12–14] These studies suggest a significant role of combined diradical and zwitterionic contributions in determining the chemical properties of the species. Despite the progress made, our understanding of the reactivity and chemical dynamics of Criegee intermediates is still very limited. Experimentally, this is due to difficulties in measuring Criegee intermediates directly, a consequence of the short lifetimes of the species under ambient conditions.

The objective of the present work is to study the chemical dynamics of Criegee intermediates by carrying out dynamics simulations on the time scale of the unimolecular processes of a simple carbonyl oxide, CH_2OO. For this purpose, it is essential to use a high-level ab initio potential that can adequately describe the possible multiconfigurational nature of intermediates in the dynamics, as well as of transition states or other geometries along the trajectories.

The possible diradical or zwitterionic character of the electronic states in the course of the dynamics is of key interest. We chose the MR-PT2 method[15] for this purpose, with Dunning's cc-pVDZ[16,17] as basis for this system, and used the software in GAMESS.[18] The application for the dynamics simulations was enabled by an accelerated algorithm we developed for simulations with MR-PT2. As described previously,[19] this method employs parallelization of the computed numerical forces. Other suitable approaches are available. For example, on-the-fly dynamics simulations with multireference potentials were carried out by Martínez and co-workers.[20,21] Coupled-cluster methods also provide an adequate multiconfigurational treatment of the wave function in the dynamics as in the EOM-CCSD study by Shepler et al.[22] For larger systems, a semiempirical approach, OM2/MRCI, is available.[23] We used a time step of 0.1 fs in our simulations.

Before proceeding to the unimolecular dynamics, it is useful to consider CH_2OO at its equilibrium structure, shown in Figure 1 a. CH_2OO has a C_s symmetry, with all atoms in the symmetry plane. In the active space, we include only 12 electrons in 11 orbitals. The s orbitals from carbon and oxygen atoms are excluded, which does not affect the CH_2OO equilibrium structure or the vibrational frequencies. The partial charges on the atoms from an NBO analysis[24] are shown in Figure 1 a. There are significant partial charges on both oxygen atoms, and a corresponding positive charge on the CH_2 group. The species has a modest zwitterionic character. The NBO analysis shows that the CO bond is a double bond, while the O–O bond is a single bond. At the equilibrium configurations, the highest CI coefficient is 0.90. This corresponds to a significant multiconfigurational char-

---

[*] J. Kalinowski, Prof. M. Räsänen, Dr. P. Heinonen, Prof. I. Kilpeläinen, Prof. R. B. Gerber
Department of Chemistry, University of Helsinki
A.I. Virtasen aukio 1 (P.O. BOX 55), 00014 Helsinki (Finland)
E-mail: jaroslaw.kalinowski@helsinki.fi
Prof. R. B. Gerber
Institute of Chemistry, The Hebrew University
Jerusalem 91904 (Israel)
and
Department of Chemistry, University of California
Irvine, CA 92697 (USA)

[**] We thank the Academy of Finland and the University of Helsinki for support of this work in the framework of the FiDiPro program. We also thank the Finnish CSC Center for the computational resources provided. R.B.G. is also supported by the Israel Science Foundation (grant 172/12) and the National Science Foundation (CHE-090-9227).

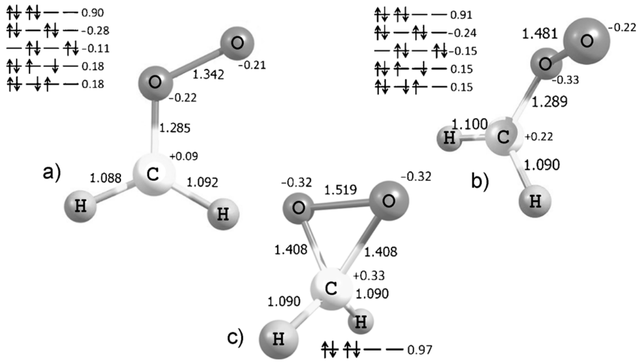

Figure 1. Minimum structure of CH_2OO (a), transition state (b) for $CH_2OO \rightarrow CH_2O_2$ decomposition, and CH_2O_2 minimum structure (c), together with corresponding main configurations of multireference wave functions together with coefficients. Numbers on the structures are bond lengths in angstroms and partial charges from NBO analysis.

acter. At least four configurations in addition to the leading one contribute significantly to the species in Figure 1 a. We note especially the diradical configurations 2 and 3 (see Figure 1 a, b), which play an important role in a subsequent transition state.

In summary, at equilibrium, CH_2OO has a significant but not very large zwitterionic character, and it has a partial, but not dominant diradical nature. This characterization is in good agreement with findings from recent ab initio studies.[12–14] To explore the unimolecular transformation dynamics of CH_2OO, we carried out a trajectory calculation using the MR-PT2 ground-state potential on the fly.

The most important decay channel for CH_2OO is arguably $CH_2OO \rightarrow CH_2O_2$, with a energy barrier of $E_b = 22.78$ kcal mol^{-1} calculated by using MR-PT2 (Table 1). The CH_2O_2 structure is shown in Figure 1 c. Comparison with CCSD(T) and higher basis sets suggest that results from MR-PT2/cc-pVDZ are reasonably accurate. The transition state (TS) is shown in Figure 1 b. In the TS, the terminal oxygen is out-of-plane. The C–O distance is almost the same as in the equilibrium structure of CH_2OO. The imaginary vibrational frequency of the TS is 894i cm^{-1}. The partial charge on the carbon atom in the TS is significantly higher than in the equilibrium structure. This may look like enhancement of the zwitterionic character on the path between the minimum energy structure and the TS, but the change corresponds only to a charge transfer between carbon and the first oxygen atom. Judging by the relatively small charge on the carbon atom, it seems that the singlet diradical character is more important for CH_2OO properties than the zwitterionic aspect.

Table 1: Comparison of energy barriers (E_b) for the $CH_2OO \rightarrow CH_2O_2$ reaction and relative energies [kcal mol^{-1}] of CH_2O_2 and $CO + H_2O$ to CH_2OO calculated by using different methods.

	cc-pVDZ	cc-pVTZ	aug-cc-pVTZ
		E_b	
MR-PT2	22.78	21.32	19.98
CCSD(T)	20.12	19.88	19.66
		CH_2O_2	
MR-PT2	−45.09	−44.93	−53.66
CCSD(T)	−46.66	−47.28	−45.98
		$CO + H_2O$	
MR-PT2	−104.37	−101.62	−102.12
CCSD(T)	−110.18	−109.24	−108.26

The barrier for the $CH_2OO \rightarrow CH_2O_2$ isomerization requires longer time trajectories if we start from the equilibrium structure. From transition-state theory, the calculated half-life for $CH_2OO \rightarrow CH_2O_2$ isomerization at 300 K is several hours. We thus began our simulations of the unimolecular dynamics from the TS between CH_2OO and CH_2O_2. The trajectories were initiated by distributing an internal energy corresponding to $T = 300$ K between the vibrational modes of the TS. We ran a total of 100 trajectories to provide sufficient statistics; the dynamics of all the trajectories is quite similar. In discussing the results we will focus on one representative trajectory.

In Figure 2, we consider snapshots from the trajectory, and describe the evolution of the dynamics from the TS in Figure 1 b. The first snapshot shows the system 39 fs after the initiation of the process at the transition-state geometry. The CO distance is now more extended, and the nature of the electronic state is changing. The contribution of the diradical configuration is lower than in the TS. At 49 fs, the system reaches geometry close to the equilibrium structure of the dioxirane molecule. It must be kept in mind that the species is very hot, since it came downhill from the transition-state structure. The leading CI coefficient is now 0.96. The dioxirane molecule itself is essentially a single-configuration, closed-shell species at equilibrium geometry. The combined charges on the oxygen atoms, −0.64, and the corresponding positive charge on the CH_2 group (+0.32 on the carbon atom) show an increased zwitterionic nature compared with CH_2O_2, and with the TS of Figure 1 b. The high kinetic energy of the species means that at $t = 2639$ fs, a hydrogen atom moves closer to the oxygen atoms. The system becomes again substantially multiconfigurational, the CI coefficient dropping to 0.91. The increased diradical nature corresponds to the fact that the large amplitude motions are due to an H atom, not a proton. At $t = 2669$ fs, the H atom is even closer to the oxygen atoms, and still bounces between them. This geometry is in the proximity of a transition state for an H atom transfer to an oxygen. The diradical character in this situation is higher than for CH_2OO, or for any of the previous geometries along the trajectory. The CI coefficient for the leading configuration is only 0.80. It can be concluded that the hydrogen transfer step in the unimolecular decay of CH_2OO, on the way to formation of formic acid structure, is the one where diradical behavior is the most strongly manifested. At $t = 2679$ fs, the H atom begins to attach to one of the oxygen atoms, and the electronic structure is now strongly dominated by the closed-shell ground-state configuration. The leading CI coefficient is now 0.97. At $t = 2837$ fs, the system is at a geometry very close to that of formic acid in its equilibrium state. However, the newly formed formic acid is very hot. The system has reached a low-energy intermediate, and the kinetic energy has built up considerably in cascading down through the previous intermediates of higher potential energy. Under

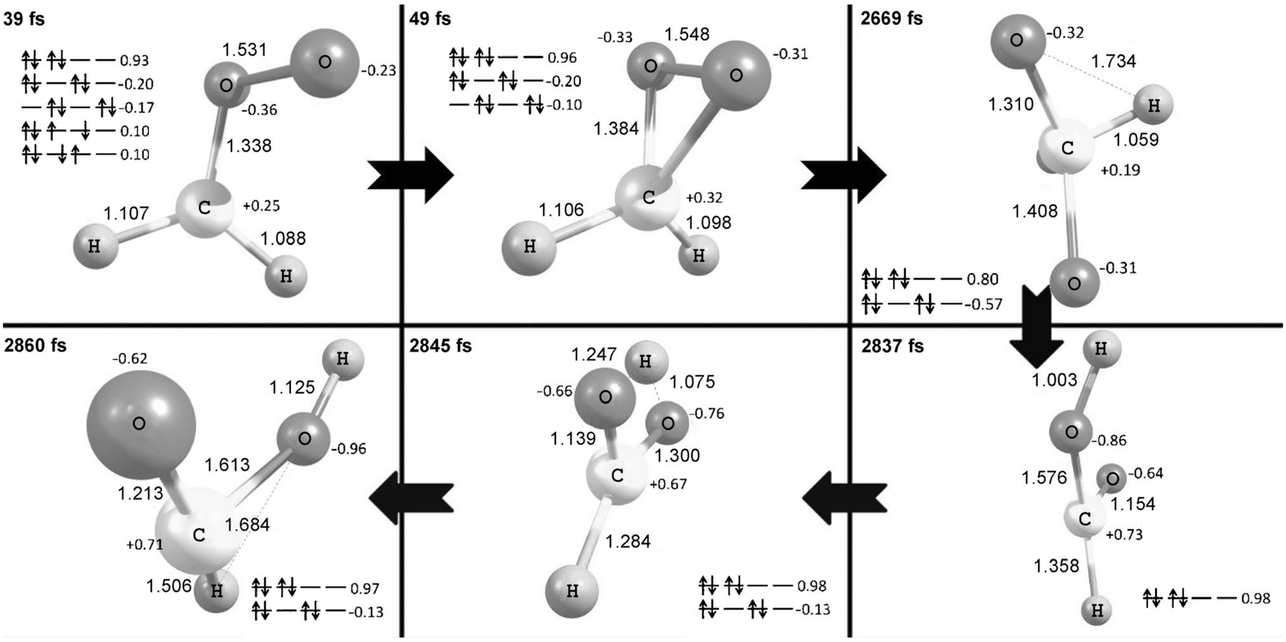

Figure 2. Snapshots from ab initio molecular dynamics simulation of thermal decomposition of CH_2OO starting from the transition structure. Main contributions to multireference wave functions are presented together with partial charges and distances in angstroms.

these conditions, formic acid can easily shuttle between *cis* and *trans* isomers. At $t = 2845$ fs, we see a proton transfer event, made possible by the kinetic energy available. Each of the trajectories computed showed two to three proton transfer events at the formic acid formation stage, that is, the proton bounces back and forth more than once before becoming firmly attached to the oxygen atom. As is often the case for proton transfer, also in this system the potential that governs the dynamics is essentially a single-configuration one. The leading CI coefficient is 0.98. However, at $t = 2860$ fs, another large motion of a proton takes place because of the high kinetic energy. The electronic state remains essentially a single-reference one. The system is now close to a transition state for decomposing into CO + H_2O, and the two products are well separated at $t = 2878$ fs (see Figure 3).

The entire dissociation process from the transition state of Figure 1 b, through the dioxirane and formic acid structures as intermediates, takes only about 3 ps. The other trajectories show very similar timescales.

Distribution of a timescale for dioxirane decay is quite narrow (Figure 4 a) with a standard deviation of approximately 80 fs. The timescale distribution for the decomposition $CH_2OO \rightarrow CO + H_2O$ is much wider, since this is a complex process that involves multiple isomerization steps. From 100 trajectories, 56 show 3 *cis–trans* transitions, 30 show 2 transitions, and 14 show one transition. For proton transfers, we observe 4 transfers in 43 trajectories, 3 in 32 trajectories, 2 in 24 trajectories, and one trajectory with one proton transfer.

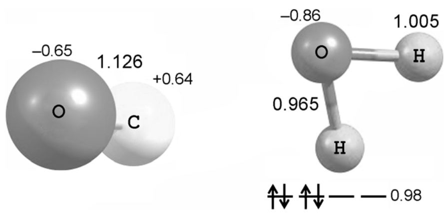

Figure 3. End of ab initio molecular dynamics simulation (2878 fs) of thermal decomposition of CH_2OO starting from the transition structure. Main contributions to multireference wave functions are presented together with partial charges and distances in angstroms.

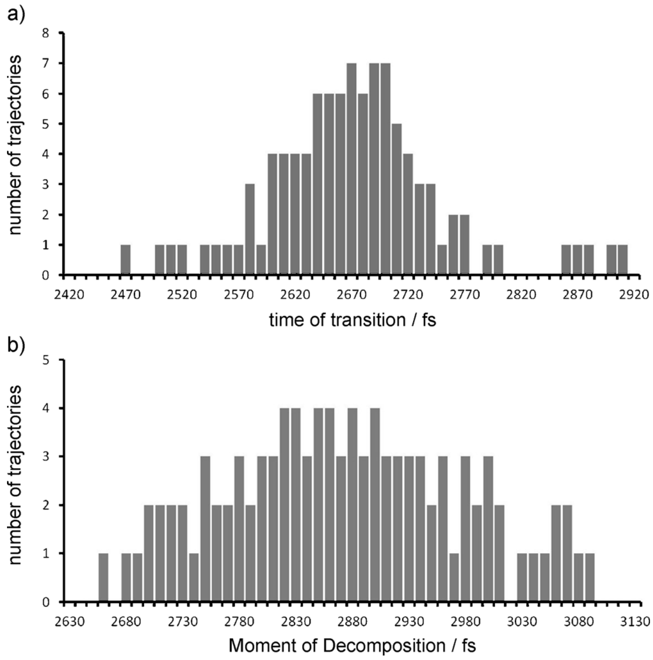

Figure 4. Statistical distribution of timescales for a) dioxirane decay formed from Criegee intermediate decomposition; b) $CH_2O_2 \rightarrow CO + H_2O$ decomposition.

This spread of the number of additional steps between formation of the formic acid intermediate and its decomposition causes also a wide distribution of the decomposition timescale (see Figure 4b). The process is extremely fast because the system is cascading down from a very high energy structure.

This conclusion has important implications for the unimolecular dynamics of Criegee intermediates. One consequence is that, in the gas phase, the dioxirane or the formic acid intermediates can only proceed to decomposition. In fact, these intermediates should only be observable by ultrafast experiments. Under typical gas-phase conditions, there is little possibility to stabilize the intermediates by collisions, as the frequency of the latter is too low. Observation of dioxirane as an intermediate was claimed in certain experiments.[25] Possibly, in these experiments, the Criegee intermediate becomes deactivated before reaching the transition state for isomerization to dioxirane, thus not contradicting our results. There may also be effects such as the presence of complexes or clusters, even in the gas phase, which may allow for deactivation even after dioxirane is formed. All these hypotheses pose fascinating challenges for future experiments.

In summary, the unimolecular dynamics of a simple Criegee intermediate were studied with ab initio molecular dynamics simulations, using a high-level multiconfigurational approach, which is essential in this case. The Criegee intermediate has both a zwitterionic and diradical character. The role of diradical configurations seems very important in particular for the hydrogen-atom transfer events leading to the formic acid intermediate. The zwitterionic configurations are important especially for events where the transferred H atom is essentially a proton. It is of interest to examine if the behavior for larger Criegee intermediates is different. The questions of formation dynamics of Criegee intermediates and of reactions of Criegee intermediates with other molecules involve related issues. On the basis of the present study, it seems that ab initio molecular dynamics suites with multiconfigurational methods, such as the MR-PT2 used here or suitable coupled cluster algorithms, should prove powerful tools for exploring these fascinating systems.

Received: August 19, 2013
Revised: October 25, 2013

Keywords: ab initio calculations · Criegee intermediates · molecular dynamics · ozonolysis · transition states

[1] R. Criegee, G. Wenner, *Chem. Ber.* **1949**, *82*, 9.
[2] D. Johnson, G. Marston, *Chem. Soc. Rev.* **2008**, *37*, 699.
[3] S. Hatakeyama, H. Akimoto, *Res. Chem. Intermed.* **1994**, *20*, 503.
[4] K. J. Heaton, R. L. Sleighter, P. G. Hatcher, W. A. Hall IV, M. V. Johnston, *Environ. Sci. Technol.* **2009**, *43*, 7797.
[5] J. H. Kroll, J. H. Steinfeld, *Atmos. Environ.* **2008**, *42*, 3593.
[6] L. J. Carpenter, *Chem. Rev.* **2003**, *103*, 4953.
[7] A. J. Eskola, D. Wojcik-Pastuszka, E. Ratajczak, R. S. Timonen, *Phys. Chem. Chem. Phys.* **2006**, *8*, 1416.
[8] O. Welz, J. D. Savee, D. L. Osborn, S. S. Vasu, C. J. Percival, D. E. Shall-cross, C. A. Taatjes, *Science* **2012**, *335*, 204.
[9] C. A. Taatjes, G. Meloni, T. M. Selby, A. J. Trevitt, D. L. Osborn, C. J. Percival, D. E. Shallcross, *J. Am. Chem. Soc.* **2008**, *130*, 11883.
[10] Y.-T. Su, Y.-H. Huang, H. A. Witek, Y.-P. Lee, *Science* **2013**, *340*, 174.
[11] M. Clay, B. S. Ault, *J. Phys. Chem. A* **2010**, *114*, 2799–2805.
[12] D. J. Cremer, *J. Am. Chem. Soc.* **1979**, *101*, 7199.
[13] D. Cremer, J. Gauss, E. Kraka, J. F. Stanton, R. J. Bartlett, *Chem. Phys. Lett.* **1993**, *209*, 547.
[14] E. Miliordos, K. Ruedenberg, S. S. Xantheas, *Angew. Chem.* **2013**, *125*, 5848; *Angew. Chem. Int. Ed.* **2013**, *52*, 5736.
[15] K. Hirao, *Chem. Phys. Lett.* **1993**, *201*, 59.
[16] T. Dunning, *J. Chem. Phys.* **1989**, *90*, 1007.
[17] D. Woon, T. Dunning, *J. Chem. Phys.* **1993**, *98*, 1358.
[18] M. Gordon, M. Schmidt, *Theory and Applications of Computational Chemistry*, the first forty years, **2005**, chap. 41, pp. 1167–1189.
[19] J. Kalinowski, M. Rasanen, R. B. Gerber, *Chem. Phys. Lett.* **2012**, *535*, 44.
[20] A. Toniolo, A. L. Thompson, T. Martínez, *J. Chem. Phys.* **2004**, *120–121*, 133.
[21] M. Ben-Nun, J. Quenneville, T. J. Martínez, *J. Phys. Chem. A* **2000**, *104*, 5161.
[22] B. C. Shepler, E. Epifanovsky, P. Zhang, J. M. Bowman, A. I. Krylov, K. Morokuma, *J. Phys. Chem. A* **2008**, *112*, 13267.
[23] D. Shemesh, R. B. Gerber, *Mol. Phys.* **2012**, *110*, 605.
[24] E. D. Glendening, C. R. Landis, F. Weinhold, *WIREs Comput. Mol. Sci.* **2012**, *2*, 1.
[25] F. J. Lovas, R. D. Suenram, *Chem. Phys. Lett.* **1977**, *51*, 453.